

## Anomalous x-ray transmission in dislocation-free silicon after electron irradiation

G. Fritsch\* and J. S. Koehler

*Department of Physics, University of Illinois at Urbana-Champaign, Urbana, Illinois 61801*

(Received 5 August 1980)

Changes in the anomalous x-ray transmission intensity upon electron irradiation of dislocation-free silicon crystals have been measured. The irradiation at 20 K produced large changes in the transmission of the [220] reflection (i.e., 5%). Some annealing experiments were done. Attempts to understand the large changes suggest that some of the point defects agglomerate forming dislocation loops during irradiation.

### I. INTRODUCTION

There has been considerable interest in the defect structure of silicon after electron irradiation. The comprehensive studies of Watkins<sup>1</sup> and collaborators led to the following picture of the defects. Several charge states of the vacancy, vacancy clusters, and vacancy-impurity clusters have been identified. Their annealing behavior and their properties have been studied in some detail. However, little progress has been made in understanding the interstitial, since, according to Watkins<sup>2</sup> and McKeighen *et al.*,<sup>3</sup> this type of defect possesses either a very low activation energy of migration or shows a mobility during irradiation. Only dopant interstitials<sup>1</sup> and eventually clusters of interstitials<sup>4,5</sup> could be seen after irradiation.

The purpose of this work was, therefore, to obtain further information on the behavior of irradiated silicon. As an experimental tool the anomalous x-ray transmission in the thick-crystal case was used, since this method is (i) sensitive to single defects (especially interstitials),<sup>6</sup> (ii) under favorable circumstances gives information on the symmetry of the defect, and (iii) is most sensitive to cluster formation.<sup>7</sup> In addition the annealing behavior of the damage-induced anomalous absorption can be studied. This is most important in order to separate the contributions from the various defects, present after irradiation, from one another.

It is known from earlier work using anomalous transmission that irradiation with fast neutrons at room temperature gives large effects,<sup>8</sup> depending on the dopant concentration and on crystal quality. However, these findings could not be interpreted readily in terms of a discrete defect structure. Therefore electron irradiation at He temperature was used in this work together with highly doped, dislocation-free single crystals. In order to get a measurable effect, high defect concentrations are required. Since the defect production seemed to be limited by saturation effects,<sup>2,3</sup> coupled to the dopant concentration, a high irradiation dose of about

$10^{18}$ – $10^{19}$   $e^-$   $\text{cm}^{-2}$  seems to be necessary in order to generate enough Frenkel pairs.

### II. EXPERIMENTAL DETAILS

The experimental setup used in this work is described in detail elsewhere.<sup>9</sup> Briefly it consists of a line-focus x-ray beam of 0.1 to 1 mm width. The anomalously transmitted intensity is detected by a scintillation counter, analyzed by an electronic window discriminator, and registered in a fast electronic counter. The intensity of the primary beam could be monitored by a second counting channel. This system is able to measure intensities to an accuracy of about 0.3%.

The sample is contained in the usual He cryostat. An exchange gas of about 1 to  $10^{-2}$  mbar pressure of helium cools the sample. For adjustment of the vertical axis the whole cryostat can be turned around. Specimen rotation around the horizontal axis used a gear system inside the He can which can be operated by a chain device from outside the Dewar. Metallized Mylar and an aluminum alloy foil served as x-ray and as electron windows. The whole cryostat could be transported and coupled to the Van de Graaff Electron Accelerator facility of the University of Illinois. A scattering foil about 1 m in front of the cryostat and a brass aperture defined the electron beam which was monitored by a Faraday cup behind the cryostat. For calibration purposes the whole cryostat could be used as a Faraday cup.

The samples were cut with a diamond saw from a Nonex Si single crystal grown by Monsanto Chemical Company. The crystal was boron doped (*p* type). Its specific electrical resistivity amounted to 0.27  $\Omega\text{cm}$  corresponding to about  $1 \times 10^{17}$  atoms/ $\text{cm}^3$ . The material was essentially dislocation free. The Si slices had a diameter of about 2.5 cm. After cutting, the Si wafers were polished with SiC powder and etched with a 1:1:1 mixture of  $\text{CH}_3\text{COOH}$ ,  $\text{HNO}_3$ , and HF. After that procedure, two circular samples (diameter  $\approx 10$  mm) were spark cut under oil out of each wafer. In order to remove surface damage, these samples were etched again with a solution 1:19 of HF and  $\text{HNO}_3$ .

for 1 to 2 min. The remaining part of the Si wafer was used as a sample holder. This procedure helped to minimize stress on the samples during the annealing and irradiation cycles. The 10-mm diameter samples were glued to the sample holder at several spots. The [111] crystallographic axis was adjusted to be perpendicular to the crystal surface in all cases. The thickness of the samples could be measured after the irradiation and annealing procedure with a micrometer.

The annealing runs were done in the same cryostat. For this purpose the liquid He flow through the sample mount was blocked by a needle valve. An electric heater allowed the sample temperature to increase to 230 K with He in the reservoir and up to 400 K without liquid He. Temperatures were measured with calibrated carbon and platinum resistors.

Three samples were measured. They are characterized in Table I. The relevant irradiation data are given in Sec. III. For easy data analysis the thick-crystal case should be used.<sup>8</sup> Hence, the quantity  $\mu_0 t \approx 20-30$ , where  $\mu_0$  is the normal linear absorption coefficient for x-rays and  $t$  the crystal thickness. Since the thickness is limited by the stopping power for electrons, only  $\text{CuK}\alpha$  radiation can be used with a crystal thickness of 1–2 mm.  $\text{MoK}\alpha$  radiation would require a sample thickness of 20 mm. 3-MeV electrons do not penetrate through a 20-mm silicon specimen.<sup>10</sup> This constraint together with the scattering geometry severely limits the access to the various Laue reflections. Only the [220] reflection could be measured. In a diamond lattice the [111] and [311] diffracted beams are accessible to measurement in principle, but they cannot be seen in anomalous transmission because their  $\epsilon_{hkl}$  value is reduced by a factor  $1/\sqrt{2}$ .<sup>11</sup> Consequently they could be seen only in the highly strained edges in sample Si(B) I-1.  $\epsilon_{hkl}$  is the ratio of the imaginary part of the scattering amplitude in the  $[hkl]$  direction to the imaginary amplitude in the forward direction. Since the anomalously transmitted intensities are very sensitive to bending of the reflecting planes, the Laue reflections from both sides of the planes were measured at the same spot of the sample. Corrections to the intensities in cases of samples Si(B) I-1 and Si(B) I-3 were applied using a theory

of Penning *et al.*<sup>12</sup> If we define

$$\delta = I_{hkl}/I_{hkl}^0 \text{ and } a = (\mu_0 t / \cos \theta) \epsilon_{hkl}, \quad (1)$$

then the following equation can be derived for the bending parameter  $P$ :

$$P = \frac{1}{2} \frac{1 + \delta - 1/a}{1 - \delta - 2/a} \times \left[ 1 - \left( 1 - 2 \frac{(1 + \delta)^2 - 2/a(1 - \delta)}{(2 + \delta - 1/a)^2} \right)^{1/2} \right], \quad (2)$$

and for the corrected intensity  $\bar{I}_{hkl}$ :

$$\bar{I}_{hkl} = \frac{I_{hkl}}{1 - 2P + 2P^2} \exp\left(\frac{-P}{a} + \frac{2a + 12}{a + 3} \frac{P^2}{12}\right). \quad (3)$$

This is true for the Laue-reflected beam. No such correction was necessary for sample Si(B) I-2.

The peak intensities of the Laue reflections corrected for bending, background, etc. are considered to be proportional to the integrated intensities.<sup>13</sup> Since the changes after irradiation and during the annealing are small, they are analyzed according to the equation<sup>6</sup>

$$I_{hkl} = I_{0hkl} \exp\left(-\mu_0(1 - \epsilon_{hkl}) \frac{t}{\cos \theta_B}\right) \times \exp\left(-(\mu_{PE}^a + \mu_{DS}^a) \frac{t}{\cos \theta_B}\right), \quad (4)$$

with  $\epsilon_{hkl} = \pi \gamma e^{(-W)} \epsilon_{0hkl}$ .

Here  $I_{hkl}$  is the intensity measured after irradiation or after annealing,  $I_{0hkl}$  describes the primary beam intensity,  $\mu_0$  is the normal absorption coefficient for the x-rays used,  $\theta_B$  the Bragg angle for the  $hkl$  reflection, and  $t$  the crystal thickness.  $\mu_{PE}^a$  and  $\mu_{DS}^a$  are the effects caused by the defects, where  $\mu_{PE}^a$  describes the photoelectric-absorption part and  $\mu_{DS}^a$  the diffuse-scattered part of the intensity.  $\pi$  is the polarization factor,  $\gamma$  equals 1 for the  $4n$  and  $1/\sqrt{2}$  for the  $(4n \pm 1)$  reflections of the diamond lattice ( $n = 1, 2, 3, \dots$ ).  $\exp(-W)$  is the Debye-Waller factor and  $\epsilon_{0hkl}$  finally gives the anomalous transmission effect (Borrmann effect). The quantities  $\mu_{PE}^a$  and  $\mu_{DS}^a$  depend on the defect parameters; they are discussed in detail in Sec. V.

### III. IRRADIATION DATA

The samples were irradiated with electrons of energy  $2.8 \pm 0.1$  MeV. They were turned around after half of the irradiation dose in order to guarantee a homogeneous defect distribution. The range of these electrons in silicon is about 3.6 mm. Hence the crystal thickness should be smaller than that figure. According to the expression given by Seitz and Koehler,<sup>14</sup> the scattering cross section for Si can be calculated once the displacement energy  $T_d$  is known. The results for 3-MeV

TABLE I. Sample characterization.

Sample	Thickness (mm)	Annealing temperatures (K)
Si(B) I-1	1.93 $\pm$ 0.02	88, 68, 238, 300, 390
Si(B) I-2	2.018 $\pm$ 0.001	105, 151, 189, 292
Si(B) I-3	1.44 $\pm$ 0.01	120, 200

electrons and  $T_d = 30$  and  $15$  eV (Ref. 3), respectively, are 31 and 64 b. These figures correspond to  $1.3$  and  $3.2$   $\text{cm}^{-1}$  or to roughly 0.3 and 0.7 defects per incident electron, respectively, for a sample thickness of 2 mm. No orientational dependence of  $T_d$  was taken into account in this calculation. Since a defect concentration of about  $10^{-4}$  is necessary, the above values imply a  $e^-$  dose of about  $2 \times 10^{18} e^-$ .

The electron flux was monitored by a Faraday cup behind the cryostat. The integrated flux was taken directly from an electronic integrator coupled to the Faraday cup. In order to get the relation between the flux measured by the Faraday cup and the flux incident on the sample, the assumption was made that all the electrons which did not leave the cryostat have been trapped by the He shield. Together with the geometry of the aperture, an enhancement factor of about 33 was derived (i.e., the sample flux is 33 times the Faraday-cup flux). This clearly is an estimate and gives an upper limit for the electron dose, since not all the electrons trapped in the He shield might have hit the sample.

The relevant values are given in Table II for all three samples measured. The He-loss rate during irradiation was about 1.8–1.9 l/h. The exchange gas pressure amounted to about  $4 \times 10^{-2}$  Torr. The irradiations were done at a nominal sample temperature of about 17 K. Sample Si(B) I-1 was accidentally heated to about 40 K after 2.13 h of irradiation, sample Si(B) I-2 to 92 K after 4.2 h of irradiation. During irradiation sample Si(B) I-3 experienced about 19 K as highest temperature. On the basis of the scattering cross section calculated above and without considering saturation effects as found by McKeighen *et al.*,<sup>3</sup> the expected single-defect concentrations are given in the last column of Table II. As discussed above, these values should be upper limits of the true single-defect concentrations.

#### IV. EXPERIMENTAL RESULTS FOR ANOMALOUS X-RAY TRANSMISSION

All measurements of transmitted x-ray intensity were taken at a temperature of 4.2 K. The angular

positions of the x-ray counter, as well as the horizontal sample axis, have been determined by adjusting to maximum intensity. This procedure was performed with the sample in reflection position at approximately maximum intensity. Data were then taken from a scan across the Laue peak using an angular rotation around the vertical axis of the sample. The counting statistics yield a statistical accuracy of the data of about 0.3%. The maximum intensities were corrected for background, measured at  $\pm 1^\circ$  relative to the peak position. In addition the data have been normalized with respect to the monitor counting rates. Dead-time corrections for the counting rate were not necessary since the changes in the counting rate from irradiation and annealing were small and the counting rates were low (less than 1 kHz). The total error of the intensities should amount to about 0.5%. Since the positioning of the beam at the sample surface affects the intensities to some extent, care was taken to adjust the cryostat after irradiation to the identical position used before. This accuracy is about 0.01 mm, hence its influence on the intensities is negligible.

The samples were tested prior to the measurements for the homogeneity of the anomalous transmitted intensity as a function of the beam positioning on the sample (locations). Results for the sample Si(B) I-2 ([220] reflection) are shown in Fig. 1. The locations for the measurements are taken from this plot as indicated. The intensity variation over several millimeters is about 1%. Hence no dislocation or elastic bending seems to be present. This statement is supported by the measurement of the scattered intensity from the  $[\bar{2}\bar{2}0]$  reflection which showed within 1% the same intensity.

The annealing runs were performed by simply heating the sample can. Therefore the heating and cooling times are not negligible when compared to the holding times of about 15 min. This is especially true for the higher annealing temperatures. Thus the changes in intensity do not correspond to the isochronal annealing method; they can only give a qualitative understanding of the annealing behavior.

TABLE II. Irradiation data for the three samples measured. The first four columns give the results for the irradiation of the front and rear side of the samples, respectively. The fifth column represents the total dose, corrected as described in the text. The last column gives the theoretically expected defect concentration.

Sample	Irradiation front		Irradiation rear		Irradiation total		Defect concentration (Calculated)
	Dose ( $10^{16}e^-$ )	Time (h)	Dose	Time	Dose	Time	
Si(B) I-1	2.67	17.2	1.87	16.82	1.5	34.02	$1.4 \times 10^{-4}$
Si(B) I-2	2.47	26.95	2.47	25.85	1.6	52.80	$1.6 \times 10^{-4}$
Si(B) I-3	2.26	20.33	2.24	20.93	1.5	40.27	$1.4 \times 10^{-4}$

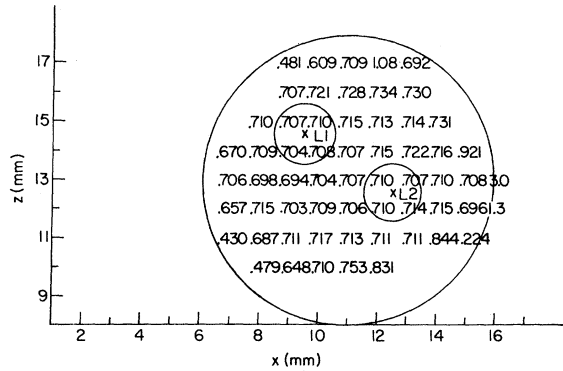


FIG. 1. Anomalously transmitted intensities for the [220] reflection as a function of the sample position. The beam diameter was 0.35 mm. The geometrical sample size is indicated approximately by the circle. The statistical counting error amounts to 0.002. The numbers given are counting rates normalized to the monitor counts. Locations  $L_1$  and  $L_2$  are indicated. The data refer to the sample Si(B) I-2.

Finally, correction for crystal bending was necessary in the runs taken with samples Si(B) I-1 and Si(B) I-3. As discussed in Sec. II, a theoretical model due to Okkerse *et al.*<sup>12</sup> was used. It turned out that the bending changed during irradiation and recovered partly during the annealing runs. The relevant parameter  $P$  [see Eq. (2)] is given in Fig. 2.

The experimental results for the [220] reflections are represented in Table III. These values are corrected as discussed above. In order to facilitate comparison with theory, the [220] data are analyzed with the help of Eq. (4) where the measured thickness (see Table I) has been used. In

addition the following quantities for Si have been used<sup>3</sup>:

$$a = 5.43 \text{ \AA}, \quad \theta_B^{[220]} = 23.68^\circ, \quad (5)$$

$$\mu_0 \text{ Cu K}\alpha = 141 \text{ cm}^{-1}, \quad \epsilon_{0[220]} = 0.964.$$

A plot of  $\mu^d = \mu_{PE}^d + \mu_{DS}^d$  as a function of the annealing temperature is presented in Fig. 3. It is interesting that the effect of the thickness in Eq. (4) is correctly reproduced in the data, since—with the exception of one location in sample Si(B) I-3—the experimental  $\mu^d$  agree very well, whereas the thickness of the samples varies by a factor of 1.4. The dependence of  $\mu^d$  on the annealing temperature is not very clear cut. On the one hand the samples Si(B) I-2 and I-3 show a rise in the transmitted intensity with increasing annealing temperature, on the other hand the data from sample Si(B) I-1 remain nearly constant.

## V. DISCUSSION

The real surprise is that such large decreases in transmitted x-ray intensity are observed upon irradiation. The average drop observed upon irradiation was 5.0%. The calculated interstitial concentration was  $C_I \approx 1.4 \times 10^{-4}$ , assuming no annihilation during irradiation. It is interesting that Edelheit *et al.*<sup>9</sup> observed for 3-MeV electrons on copper crystals irradiated at 20 K a decrease in the [220] transmitted intensity of 4.1% when the calculated interstitial concentration was  $C_I \approx 1.2 \times 10^{-4}$ . So the changes are comparable.

There are at least two possibilities. First, the interstitials and vacancies may be present in the silicon as isolated point defects. This would re-

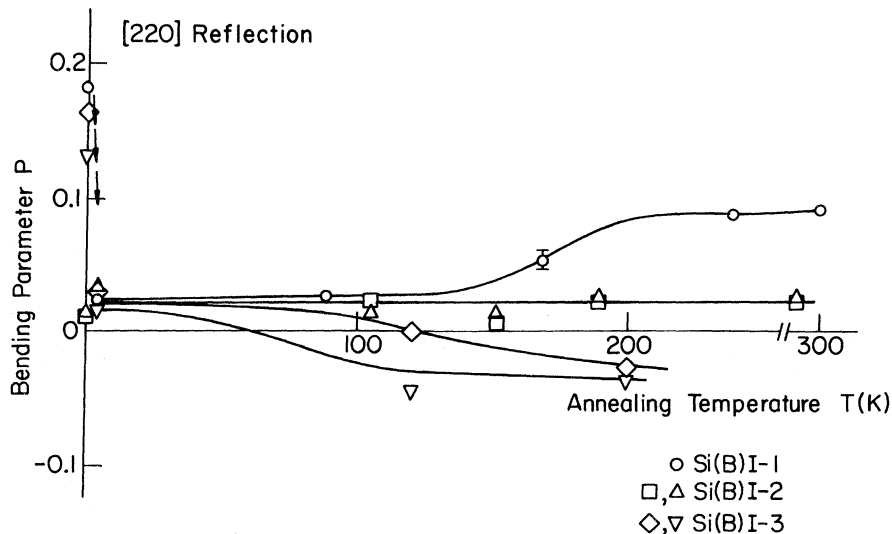


FIG. 2. Bending parameter  $P$  for the [220] reflections derived from the measured intensities from the [220] and  $\bar{2}\bar{2}0$  reflections according to Okkerse *et al.* (Ref. 12). Data are given as a function on the annealing temperature or the various samples measured. The lines are only guides to the eye.

TABLE III. Intensity ratio  $R$  of the anomalous x-ray transmission for the [220] for various samples and annealing temperatures. The numbers given are the ratios of the normalized peak intensities after irradiation to those before.  $L_1, L_2$  indicate the various locations measured.

$R = \frac{\text{normalized } I_{\max} \text{ after treatment}}{\text{normalized } I_{\max} \text{ before treatment}}$						
Sample	$R$ after irradiation		$R$ after irradiation plus anneal at $T$ (K)			
Si 1	0.933	0.938	168 K	238 K	300 K	390 K
Si(B) 2/ $L_1$	0.922	0.950	105 K	151 K	189 K	292 K
Si(B) 2/ $L_2$	0.942	0.955	0.951	0.933	0.901	
Si(B) 3/ $L_1$	0.985	0.971	120 K	200 K	0.954	
Si(B) 3/ $L_2$	0.964	0.951		0.932		

quire that either the interstitial or the vacancy or both had a large lattice distortion associated with them. Or, second, it is possible that either the interstitial or the vacancy or both migrate athermally during irradiation. In this case the large transmitted intensity change results from the formation of dislocation loops. Young *et al.*<sup>6</sup> and Dederichs<sup>7</sup> give theoretical results which predict the influence of point defects and of dislocation loops on the photoelectric-absorption (PE) coefficient  $\mu_{\text{PE}}^d$  and on the defect contribution to the diffuse-scattering (DS) absorption coefficient  $\mu_{\text{DS}}^d$ .

First let us consider point defects. We have made calculations biased towards giving large single-defect contributions. We take  $C = C_I = 1.5 \times 10^{-4}$  (see Table I), and we assume a large volume change resulting from the interstitial,<sup>15</sup> i.e.,  $V_d = V_0$ , where  $V_0 = 20.01 \text{ \AA}^3$  is the atomic volume. Young, Baldwin, and Dederichs<sup>6</sup> give

$$\mu_{\text{PE}} = \mu_0 L_h + \mu_0 C_I (1 - \cosh \vec{h} \cdot \vec{R}_I), \quad (6)$$

where  $h$  is the reciprocal-lattice vector and  $R_I$  gives the location of the interstitial atom measured from a perfect lattice position.  $L_h$  describes

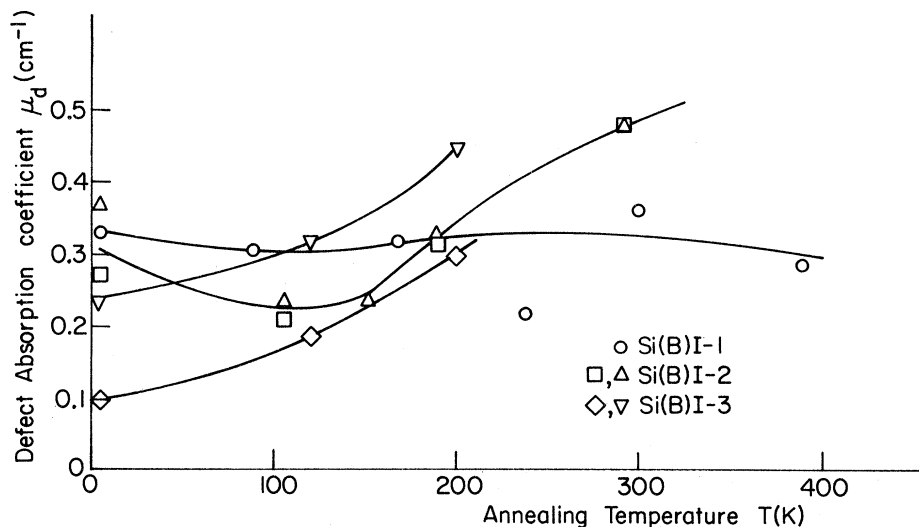


FIG. 3. Defect absorption part for the anomalously transmitted intensities  $\mu_d$  according to Eq. (4). The data refer to the [220] reflections for the various samples and locations.

the effect of the long-range strain field around the interstitial. Young *et al.*<sup>6</sup> find

$$L_h = C_I \left( \frac{V_d}{V_0} \right)^2 \left( \frac{1+\nu}{1-\nu} \right)^2 \frac{h^2 V_0}{P_c}. \quad (7)$$

In Eq. (7)  $P_c$  is an inner cutoff radius ( $P_c = 1.2 \times 10^{-10}$  m).  $h^2$  is the square of the magnitude of the reciprocal-lattice vector (for [220]),  $|\vec{h}| = 3.273 \times 10^{10} \text{ m}^{-1}$  or  $h^2 = 10.712 \times 10^{20} \text{ m}^{-2}$ ).  $\mu_0$  is the linear absorption coefficient which amounts to  $141 \text{ cm}^{-1}$  for CuK $\alpha$  radiation and  $\nu$  is Poisson's ratio ( $\nu = 0.38$  for Si).<sup>6</sup> In the case of vacancies  $C_v$  replaces  $C_I$ . The term  $\mu_0 C_I (1 - \cosh \vec{h} \cdot \vec{R}_I)$  in Eq. (6) disappears, since no additional atom is present.

Dederichs<sup>7</sup> gives the diffuse scattering absorption coefficient for dislocation loops of radius  $R_0$  and Burgers vector  $\vec{b}$  to be

$$\mu_{\text{DS}} = \frac{C_I}{V_0} (\nu_0 f_h)^2 \left( \frac{h}{k} \right)^2 n_L \ln(q_c R_0)^{-1} \times \frac{8}{15} \left( 1 + \frac{3\nu^2 + 6\nu - 1}{6(1-\nu)^2} \cos^2 \theta_B \right), \quad (8)$$

where  $\nu_0$  is the classical electron radius ( $\nu_0 = 1.818 \times 10^{-15}$  m),  $f_h$  describes the atomic scattering factor for x rays ( $f_{[220]} = 8.665$  for Si) and  $n_L$  is the number of point defects in the loop. The latter quantity is taken to be one for the single interstitial, in general it is given by  $n_L = b \pi R_0^2 / V_0$ . Whereas  $\theta_B$  is the Bragg angle corresponding to the [220] reflection ( $\theta_B = 23.68^\circ$ ),  $q_c$  is a cutoff quantity defined by<sup>7</sup>

$$q_c = (4\pi \nu_0 f_h' / V_0) / h. \quad (9)$$

Equation (9) yields  $q_c = 4.6852 \times 10^5 \text{ m}^{-1}$  in our case.

For single interstitials we take  $\cosh \vec{h} \cdot \vec{R}_I = -1$ . Then we get from Eqs. (6) and (7)  $\mu_{\text{PE}}^I = 0.070 \text{ cm}^{-1}$ . Using Eqs. (8) and (9) with  $R_0 = 2.35 \times 10^{-10}$  m, which is the next-neighbor distance and  $n_L = 1$ , we find  $\mu_{\text{DS}}^I = 0.001 \text{ cm}^{-1}$ . Hence for single interstitials under most favorable conditions

$$\mu^I = \mu_{\text{PE}}^I + \mu_{\text{DS}}^I = 0.071 \text{ cm}^{-1}.$$

For isolated single vacancies the situation is quite different, since only the first part of Eq. (6) survives. Equation (7) can be used as it stands. However, in order to check how good this approximation is, we used, in addition to Eq. (7), the following equation for  $L_h$ , restricting the sum to the four nearest neighbors only:

$$L_h = C_v \sum_{n=1}^4 [1 - \cos(\vec{h} \cdot \vec{t}_n)]. \quad (10)$$

The quantities  $\vec{t}_n$  describe the displacements of the nearest neighbors due to the presence of a

vacancy. A tetragonal distortion as caused eventually by the Jahn-Teller effect, was applied together with an additional radial component.<sup>1,16</sup> This assumption allows one to express the displacements  $\vec{t}_n$  in terms of a single parameter  $\delta = (d - d')/d$ , where  $d$  is the nearest-neighbor distance without and  $d'$  the one with relaxation. As an example the displacement vector<sup>17</sup> is given by  $\vec{t} = (a/4)\delta(-1, -1, 0)$  in case of the nearest neighbor located at  $\vec{R} = (a/4)(1, 1, 1)$ . The third component is not important since  $\vec{t}$  is multiplied by  $\vec{h}_{220}$ . Summing up the four nearest neighbors we get  $L_h = 2C_v(1 - \cos 2\pi\delta)$ . A value of  $\delta \approx 0.16$  seems to be reasonable.<sup>1</sup> A maximum figure would be  $\delta \approx 0.5$ . We evaluated  $\mu_{\text{PE}}^v$  for the two  $\delta$ 's, using Eq. (10) and for  $\Delta V_d/V_0 = 0.1$  (1.0) with the help of Eq. (6), yielding  $\mu_{\text{PE}}^v = 0.085, 0.021, \text{ and } 0.002$  ( $0.028$ )  $\text{cm}^{-1}$ , respectively. Since  $\mu_{\text{DS}}^v = \mu_{\text{DS}}^I$ , it is easily recognized that under most favorable circumstances the effect of the isolated single vacancy is similar to or smaller than the one of the interstitial.

Watkins<sup>1</sup> has shown that boron interstitials are present after electron irradiation. Our samples were doped with a boron concentration of about  $2 \times 10^{-6}$ . A calculation yields  $\mu^B \approx 2 \times 10^{-5} \text{ cm}^{-1}$ .

Since for specimen Si(B) I-3 one observes a decrease of 2.6% in the x-ray transmission intensity upon irradiation, one can calculate  $\mu^d$  to be [see Eq. (4)]

$$\mu^d = 0.17 \text{ cm}^{-1}$$

in the worst case. The other specimens give  $\mu^d = 0.3 \text{ cm}^{-1}$ . Therefore single defects do not give the observed effect. They yield, at most, results which are too small by a factor of about 3. Consequently they would predict changes in the transmitted intensity which should be smaller by  $e^3 \approx 20$ . However, small dislocation loops can produce the necessary absorption. Young, Baldwin, and Dederichs<sup>6</sup> derive for loops

$$\mu_{\text{PE}} = \mu_0 C_L (R_0^3 / V_0)^{1/2} (hb)^{3/2} + \mu_0 C_I (1 - \cosh \vec{h} \cdot \vec{R}_s), \quad (11)$$

where  $C_I = C_L n_L$ . As already defined above,  $C_I$  is the total interstitial concentration and  $n_L$  is the number of interstitials in the loop, whereas  $C_L$  gives the loop concentration.

For a loop radius of  $R_0 = 4 \times 10^{-10}$  m and therefore  $n_L = 6$ , we get  $C_L = 2.5 \times 10^{-5}$ . Finally, we find from Eqs. (8), (9), and (10)  $\mu_{\text{PE}}^{\text{loop}} = 0.165 \text{ cm}^{-1}$  and  $\mu_{\text{DS}}^{\text{loop}} = 0.004 \text{ cm}^{-1}$  so

$$\mu^{\text{loop}} = \mu_{\text{PE}}^{\text{loop}} + \mu_{\text{DS}}^{\text{loop}} = 0.169 \text{ cm}^{-1},$$

which is about right. The value can be changed by slight variations of  $R_0$ .

Note in both calculations we have assumed that

none of the defects are annihilated, i.e., we took  $C_I = 1.5 \times 10^{-4}$  which represents the total damage production. If we assume that only a quarter of the interstitials survive, then a larger loop radius is required. Hence if  $C_I = 3.7 \times 10^{-5}$  and we take  $R_0 = 15 \times 10^{-10}$  m,  $n_L = 83$  then

$$\mu^{\text{loop}} = 0.170 \text{ cm}^{-1}.$$

Föll<sup>5</sup> has seen clusters in the electron microscope after electron irradiation at 20 K, but his fluence was  $3.6 \times 10^{22} e^-/\text{cm}^2$ , i.e., about four orders of magnitude larger than ours.

Let us consider how our results fit in with the electron paramagnetic resonance observations of Watkins.<sup>1,2</sup> He finds isolated boron interstitials after electron irradiation. His boron interstitials are supposed to be isolated up to room temperature. If his observations and ours are both correct, then some silicon interstitials go to substitutional boron atoms and others cluster. From our boron concentration of  $2 \times 10^{-6}$ , we conclude that only a minor part of the interstitials is used for boron interstitial production. Hence small interstitial loops should be present. The mechanism responsible for cluster nucleation is unknown. The fact that the decrease upon irradiation observed in sample Si(B) I-3 is smaller than the decreases seen in the other samples may be because Si(B) I-3 had no warm-up after starting the irradiation procedure (see Sec. III). Clusters produced by the heating cycle may just grow larger and produce a bigger effect than many small ones since the effect is proportional to  $c_I n_L$  [Eqs. (8)

and (11)]. This was the reason for using sample Si(B) I-3 for the calculations presented in this section.

It is difficult to explain the annealing behavior. The general trend seems to be that the absorption effect [especially Si(B) I-2, 3] increases with temperature. This can be either due to an increasing cluster size or to a nucleation of other loops, including those of vacancy type. Hence one could propose the growth of some interstitial loops at the expense of smaller ones or the nucleation of vacancy loops around a temperature of about 160 K according to Watkins.<sup>1,2</sup> In any case, one is forced to believe that, if the vacancies become mobile at 160 K their clustering must dominate their annihilation with interstitials.

## VI. CONCLUSION

The large changes observed in the anomalous x-ray transmission of silicon during electron irradiation at 20 K mean either that the point defects have a very large distortion associated with them, or that the point defects agglomerate during irradiation forming dislocation loops.

## ACKNOWLEDGMENT

Research supported by the U. S. Department of Energy under contract DE-AC02-76ER01198. We would like to thank Mr. J. Watson for help during the irradiation procedure. In addition we thank Mr. B. Clymer for help with the irradiation.

\*Present address: Physics Department, Hochschule der Bundeswehr, Munchen, 39 Werner Heisenberg St., Neuberg, Germany, 8014.

<sup>1</sup>G. D. Watkins, in *Lattice Defects in Semiconductors—1974*, edited by F. A. Huntley (The Institute of Physics, London, 1975), p. 1.

<sup>2</sup>G. D. Watkins, *J. Phys. Soc. Jpn.* **18**, Suppl. II, 22 (1963).

<sup>3</sup>R. E. McKeighen and J. S. Koehler, *Phys. Rev. B* **4**, 462 (1971).

<sup>4</sup>J. M. Pankrate, J. A. Sprague, and M. L. Rudee, *J. Appl. Phys.* **39**, 101 (1968).

<sup>5</sup>H. Föll, in *Lattice Defects in Semiconductors—1974*, edited by F. A. Huntley (The Institute of Physics, London, 1975), p. 233.

<sup>6</sup>F. W. Young, Jr., T. O. Baldwin, and P. H. Dederichs, in *Vacancies and Interstitials in Metals*, edited by A. Seeger, D. Schumacher, W. Schilling, and J. Diehl (North-Holland, Amsterdam, 1969), p. 619.

<sup>7</sup>P. H. Dederichs, *Phys. Rev. B* **1**, 1306 (1970).

<sup>8</sup>T. O. Baldwin and J. E. Thomas, *J. Appl. Phys.* **39**,

4391 (1968); R. Colella and A. Merlini, *Phys. Status Solidi* **14**, 81 (1966).

<sup>9</sup>L. S. Edelheit, J. C. North, J. G. Ring, and J. S. Koehler, *Phys. Rev. B* **2**, 2913 (1970).

<sup>10</sup>M. J. Berger and S. M. Seltzer, *Tables of Energy Losses and Ranges of Electrons and Positrons*, NASA Publication SP-3012 (1964).

<sup>11</sup>G. Hildebrandt, *Phys. Status Solidi* **15**, K131 (1966).

<sup>12</sup>B. Okkerse and P. Penning, *Philips Res. Rep.* **18**, 82 (1963).

<sup>13</sup>P. B. Hirsch, *Acta Crystallogr.* **5**, 176 (1952).

<sup>14</sup>F. Setiz and J. S. Koehler, in *Solid State Physics*, edited by F. Seitz and D. Turnbull (Academic, New York, 1956), Vol. 2, p. 307.

<sup>15</sup>J. C. North and R. C. Buschert, *Phys. Rev.* **143**, 609 (1966); *J. Appl. Phys.* **37**, 639 (1966).

<sup>16</sup>N. O. Lipari, J. Bernholc, and S. T. Pantelides, *Phys. Rev. Lett.* **43**, 1354 (1979).

<sup>17</sup>E. Kauffer, P. Pecheur, and M. Gerl, *Rev. Appl. Phys.* **15**, 849 (1980).